Changes in pore characteristics of travertines from Spišské Podhradie after repeated freeze-thaw cycles

Martin Maľa[1], Vladimír Greif[1], Martin Ondrášik[2] & Anna Macková[1]

[1] Department of Engineering Geology, Hydrogeology and Applied Environmental Geophysics, Faculty of Natural Sciences, Comenius University in Bratislava
[2] Department of Geotechnics, Faculty of Civil Engineering, Slovak University of Technology in Bratislava

AGEOS

Abstract: This study aims to understand the effect of frost weathering of travertines from Spišské Podhradie in Slovakia. The application of travertine as a natural building and facing stone shows a gradually increasing trend in construction sector around the world. Travertines are commonly seen in tile sizes as façade material, wall cladding or flooring and are naturally exposed to the freeze–thaw processes. Methods of frost damage assessment in rocks are commonly based on parameters acquired mainly by destructive testing of samples, such as the uniaxial compressive strength test or Young's modulus test. In the presented research, a nondestructive method taking advantage of selected petrophysical properties compared before and after 100 freeze-thaw (F-T) cycles, as well as recorded length change behavior and temperature development by a specially- constructed thermodilatometer (VLAP 04) with two induced linear variable differential trans- former sensors (HIRT- LVDT) on vacuum-saturated samples has been conducted. Results demonstrate that travertine from Spišské Podhradie is quite heterogeneous in term of petrophysical properties. This heterogeneity can significantly affect the nature and intensity of the processes which take place during the ice crystallization within the pore space of the rock. While crystallization pressures in the macropores and the hydraulic pressure induced by the migration of water towards the advancing freeze front cause the specimen to expand, they are not sufficient to overcome the reduction of pore pressures in micro and mesopores and thus the total contraction of the specimen occurs after 100 freeze-thaw (F-T) cycles. The changes in the microstructure of the pore space of the travertine from Spišské Podhradie are not significant and so we can state that this travertine is a resistant material to the effects of frost weathering.

Key words: travertine, frost weathering, petrophysical properties, ice crystallization, crystallization pressure, frost shrink-ing, freeze-thaw

1. INTRODUCTION

Thermally induced irreversible process in hard rocks are es-sential factor influencing landscape, natural building stones, concrete and historical masonry. One of such process is frost weathering induced by freeze-thaw action inside the pore sys-tem of the rock. These processes are closely related to both the daily and seasonal temperature oscillations, and their relevance increases especially with the climate change (Grossi et al., 2007 in Ruedrich et al. 2011). The influence of F-T (freeze-thaw) cycles on the structural performance degradation of hard rocks has been previously reported by several authors. When the temperature drops below the freezing point, moisture bear-ing materials will be subjected to internal stresses caused by the phase transition from water to ice (Winkler, 1968). These stresses are consequently released during thawing (Deprez et al., 2020). However, the mechanism of stress generation within the rock fabric due to ice crystallization is still under discus-sion. Damage induced by F-T (freeze-thaw) action is presently mainly attributed to crystallization pressure (Everett, 1961; Scherer, 1999; Steiger, 2005[a], 2005[b]; Walder and Hallet, 1985), also, volumetric expansion (Hirschwald, 1908) and hydraulic pressure theory (Powers, 1945). Crystallization pressures (Scherer, 1999, Scherer and Valenza, 2005) are caused by the crystal's will to grow in thermodynamical disequilibria. This eagerness to grow and the presence of a nanometer thick liquid

layer between the crystal and the pore wall will cause that the crystal will indeed exert pressure on the pore wall. The growing crystals will also draw unfrozen water towards them (Everett, 1961), a process is called cryosuction.   Recent research has also showed that crystallization pressures are most likely to cause damage to natural building stones (De Kock et al., 2015). According to Powers (1949) hydraulic pressures are indirectly caused by the 9 % volume expansion that accompanies the water-ice phase transition.   As water crystallizes first in the larger pores of the system in a fast manner, the 9 % volume expan-sion causes part of the water in these larger pores to be forced out into the smaller neighboring pores. Hence, if this expelled water cannot find a pore large enough to relief this pressure, hydraulic pressures build up and can damage the material. The theory of linear growth pressure as the main process of stress development within porous rocks has been discussed previously by several authors (Scherer, 1999; Steiger, 2005; Ruedrich and Siegesmund, 2007). Ruedrich et al. (2011) emphasized the significance of long-term tests in contrast to commonly per-formed standard tests, which normally include only 30–40 F-T cycles and also importance of water saturation in the damage caused by F-T cycling (Ruedrich and Siegesmund, 2007). The saturation in turn depends on various material properties, such as mineralogical composition (Dunn and Hudec, 1996) and petrophysical properties - the porosity, pore size distribution or permeability (Everett and Haynes, 1965; McGreevy, 1982;

Prick, 1995). Other important material parameters that co-define F-T resistance are mineral composition, tensile strength, and anisotropy (Nakamura et al., 1977). In this study we were working with travertines from Spišské Podhradie (Slovakia). Travertines are worldwide employed as a building stones and in civil constructions from ancient times until present (Pentecost, 2005). It has been used as structural stone and also in ornamental elements such as sculptures. Travertine is commonly seen in tile sizes as façade material, wall cladding and flooring (Demirda, 2013; Chentout et al., 2015) and so they are naturally exposed to F-T process. Durability of travertines was studied by several authors (Yavuz and Topal, 2007; Yu and Oguchi, 2010; Zalooli et al., 2017) and they showed that travertine is relative durable material. However, in outdoor environments they can undergo significant physical weathering due to salt crystallization, F-T and thermal shock action, all depending on the regional climate. Thermal stress induced by thermal cycles may be in carbonate rocks like travertines determinant because calcite has a highly anisotropic thermal dilatation (Nye, 1972). There is a connection between both thermal, ice and salt crystallization decay mechanism (Benavente et al., 2018).

2. MATERIAL AND METHODS

2.1. Rock specimens

Nine rock cores of 51 mm ±1 mm in length and 32 mm ±1 mm in diameter were cut and machined from specimen blocks collected at Spišské Podhradie (further SP(T)) (Fig. 1).

2.2. Case study area

Specimens were collected from a part of travertine mound called Perun´s rock on which Spis Castle is situated. Spis Castle is a monument inscribed on the UNESCO World Heritage Site list since 1993. Travertine mound is overlying softer Paleogene rocks which causes lateral spreading resulting from strong upper travertine's

subsidence into soft claystone strata, which has fractured and separated the castle bedrock into several cliffs. The differential movement of individual cliffs is influencing the instability of the castle rock.

2.3. Rock fabric and mineralogical structure

Rock fabric is one of the main factors controlling the petrophysical properties and their material behavior during the weathering process. Mineral content analyses were performed by SEM- Scanning Electron Microscopy of standard thin sections. These travertines are mostly white, off-white less yellow in color, amorphous or very fine-grained with a uniform grain size. The mineralogical composition of SP(T) travertine consists mainly of calcite (99 %), which is the main rock-forming mineral. Flourites or Cryptomelanes can occur as accessory minerals (Fig. 2).

3. EXPERIMENTAL APPROACHES

3.1. Porosity

Various researchers have previously reported petrophysical properties as being important rock parameters that significantly affect a rock's resistance to frost. To provide detailed information about

Fig. 1: Map of sampling location
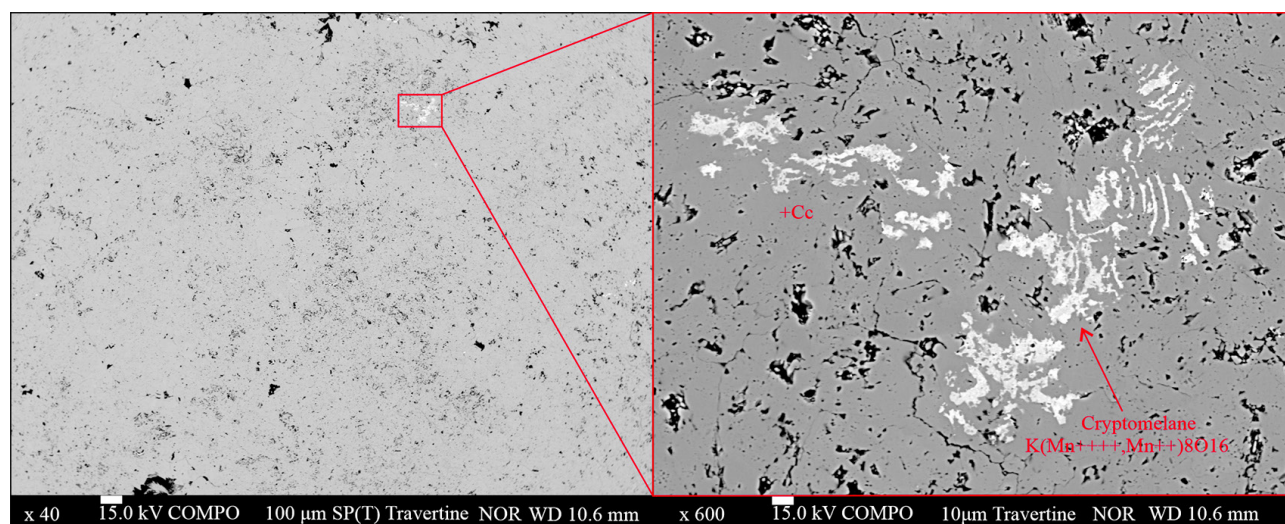
Fig. 2: SEM photos of SP(T) travertine

these parameters, we applied experimental non-destructive methods, as well as standard procedures described in EN 1936 (2007). This standard defines *inter alia* the methodological procedures applicable for the determination of bulk density, total porosity, and pore size distribution.

The standard particle density tests using Gay-Lussac glass pycnometers were carried out on all rock samples according to STN 72 1011 (1982). Rocks were pulverized in a grinder and mill for this purpose.

Effective porosity was analyzed by the pycnometric method, which is described as helium pycnometry. Helium is used in helium pycnometers to determine the particle density (or specific weight) of pulverized samples. Helium pycnometer was applied to determine rocks' open porosity (Operator manual 2005). It is similar to the technique used to measure foam polymers' open porosity (rigid porous plastics) (Adamcova, 2012). The measurement is based on the Archimedes principle; however, water is substituted by inert technical high-purity helium replaced by the sample volume V_x in the test chamber. After putting a cylinder-shaped rock sample into the chamber of a known volume of V_C, gas is let in until the required pressure is achieved. When the inlet is closed, gas penetrates all effective pores of the rock or other porous samples until the equilibrium pressure p_1 is reached. After opening the vent to an additional chamber of a known volume of V_A, helium expands and pressure drops until a new equilibrium at the pressure p_2 is reached, based on the equation: $p_1.V_1 = p_2.V_2$ (Eq. 1) (Boyle 's law of gas expansion). The volume of a solid object can be calculated from this equation as a function of the ratio p_1: p_2. A custom evaluation method using a precise calibration curve was developed. For rock sample testing, calculated volume V_x represents the solid phase volume (without helium-accessible pores, i. e. helium-effective pores). However, closed pores were included in V_x. Afterwards, the volume of the effective pores were calculated as $V_{ef}He = V - V_x$ (Eq. 2), where V is the total or "envelope" volume. Regularly shaped cylindrical samples were used, and volume V was calculated from their dimensions. Prior to each sample measurement, the sample was washed intensively by helium flow. One measurement is interpreted from the mean of 10 steady ratios p_1: p_2, with maximum deviation of $\pm$ 0,001.

3.2. PORE SIZE DISTRIBUTION
- -
For the identification of the rock pore structure and its change prior to and after testing, two different methods were used. A representative pore radii distribution was measured by standard mercury intrusion porosimetry based on STN 72 1011 (1982) in addition to a newly developed, experimental, indicative rock pore structure identification method (Ondrášik et al., 2017; Ondrášik et al., 2018). The new method assumed that water sorption (adsorption and absorption) into rock pores is controlled by the rock pore structure itself, and thus water sorption under controlled conditions determines the rock pore structure. The controlled conditions were achieved by three different suction tests: 72 h water vapor adsorption at 98 % relative humidity (further RH), 48 h water absorption under atmospheric pressure, and 24 h vacuum water absorption. In this way, four different rock pore types can be identified according to their size and accessibility to water: (Eq. 3)

micropores and mesopores (Eq. 4), easily-accessible macropores (Eq. 5), partially accessible macropores, and (Eq. 6) closed pores of any size. The pore size classification of micropores, mesopores, and macropores is the one used by the International Union of Pure and Applied Chemistry (Sing et al. 1985). The main advantage of this method is its non-destructive character, as well as its ability to be applied repeatedly prior, during, or after rock testing. A 72-hour water vapor adsorption test at 98 % RH was performed to identify the content of micropores and mesopores in the rock samples. Prior to the adsorption test, the samples were dried in an air circulating oven at 105 °C and weighed with the accuracy of $\pm$0.001g. Dry samples were put into airtight chamber with 98 % RH and constant temperature (21 °C). The 98 % RH was maintained by using a super saturated solution of hydrated copper sulphate- $CuSO_4.5H_2O$, (Weast, 1973). After 72 hours, the samples were individually weighed without removal from the climatic chamber. From the rock weight difference, the content of adsorbed water micropores and mesopores was calculated according to equation (Eq. 3).

A 48 h water absorption test made according to EN 13755 (2003) was used to identify macropores easily accessible to water. A 24 h water vacuum absorption test was further performed in order to identify macropores hardly-accessible to water. Finally, the content of closed pores was identified from the rock's total porosity determined according to EN 1936 (2007)

To calculate the content of micropores and mesopores (N_{ADS}), as well as easily-accessible macropores (N_{BULK}), hardly-accessible macropores (N_{VOID}), and closed pores of any size (N_C) from the test results, the following equations were used:

$$N_{ADS} = N_{AD98} \qquad [\text{wt. \%}] \qquad (Eq\ 3.)$$
$$N_{BULK} = N_{48} - N_{AD98} \qquad [\text{wt. \%}] \qquad (Eq\ 4.)$$
$$N_{VOID} = N_V - N_{48} \qquad [\text{wt. \%}] \qquad (Eq\ 5.)$$
$$N_C = n \cdot \frac{\rho_w}{\rho_d} - N_V \qquad [\text{wt. \%}] \qquad (Eq\ 6.)$$

where N_{AD98} is the content of adsorbed water, N_{48} is the content of absorbed water after 48 h saturation, N_V is the content of water saturated into pores by vacuum, n is the total porosity in vol. %, ρ_w is the density of water, and ρ_d is the apparent density of dry rock.

3.3. Pore connectivity by spontaneous imbibition method
- -
The method of spontaneous imbibition is a simple, nondestructive test procedure for determining the pore connectivity of rocks, which is an important topological parameter of pore systems. During the test, one face of the sample is exposed to water while measuring the mass of water uptake over time (Hu et al., 2001) (Fig. 3). This exploits the analogy with diffusion, where in homogeneous materials (excluding gravitational effects), the distance to the wetting front increases with the square root of time $l \sim t^{0.5}$. In this work, a modified testing procedure from the one employed by Hu et al. (2001) was adopted to mitigate for errors due to buoyancy force or effect of evaporation in such a way that the specimens were tested in a larger water tank compared to the Petri dish as done by Hu et al. (2001). Furthermore, test core samples were wrapped in polyethylene foil (further PE
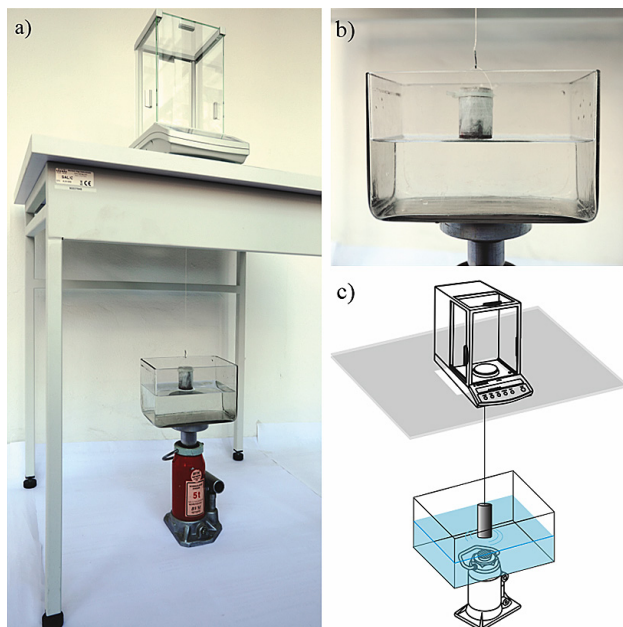
Fig. 3: Overall view of the equipment used for spontaneous imbibition tests (a) with details of the water tank placed on the jack (b) and schematic drawing of the test arrangement (c)

foil) except for the surface exposed to water in order to avoid evaporation losses. All tests were carried out on 9 specimens. Specimens were dried at 105 °C for 48 hours and then wrapped in PE foil, except for the base of the core sample, including the 1 mm side wall exposed to water in order to avoid evaporation losses. Samples were than stored in a desiccator and tested suspended under a balance with automatic reading and storage of data every 1 second for the duration of 15 minutes. A glass water reservoir with dimensions of 202 x122 x125 mm filled with water up to a height of 65 mm was placed on a supporting jack to bring the rock specimen in contact with the distilled water in the reservoir; the sample was then submerged to a depth about 1mm (Fig. 4). The temperature was maintained at 23.0 ± 1 °C. All imbibition tests (SI) were carried out in triplicate on the same sample. Samples were dried at 105 °C for 48 hours between tests. Each test was analysed by plotting the cumulative imbibition height (mm) against the square root of time (min) in the log scale. The apparent slope of a linear regression curve C(I) gives the imbibition slope characterizing speed of water imbibition into the sample. This relation, which is originally based on Handy`s model (1960), is valid only for small size samples
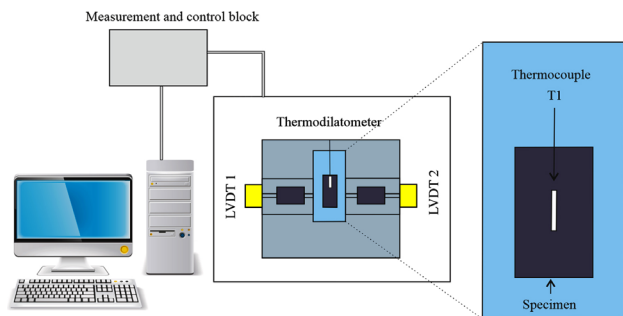
Fig. 4: Schematic drawing of the thermodilatometer VLAP04

where the effects of gravity are minimal so does the case here. As shown in Fig. 4, owing to the great variability in porosity of rock samples, the imbibition slopes varied significantly; therefore, two distinct imbibition slopes were determined separately for the time intervals 0.1–1 min and 1-10 min: imbibition slopes for the fast 0.1–1 min interval were marked for the initial state, and after 100 F-T (freeze-thaw) cycles. Slopes in the medium time range 1–10 min were marked and respectively.

3.4. Freeze-Thaw test

After completion of SI testing, the specimens were unwrapped, dried at 105 °C for 24 hours, their weight was measured, and then they were vacuum-saturated with distilled water for 48 hours to obtain maximum water saturation. The samples were further weighed, wrapped in PE foil to prevent evaporation, and placed inside the thermal chamber of the thermodilatometer, VLAP04 (Fig. 4). The VLAP04 used for the frost damage test is able to control the temperature in the range from –17 °C to + 60 °C. A control thermocouple of the thermal chamber was placed along the central rotational axis of the cylindrical dummy sample made of the same material as the tested specimens, and the temperature was cycled from –10 °C to + 10 °C. Specimens were subjected to 100 F-T (freeze-thaw) cycles with a cooling rate of –0.18 °C/min and a heating rate of 0.21 °C/min. The length change of the specimens was measured using two LVDT (linear variable differential transformer) sensors HIRT-LVDT-T101 F with accuracy of $\pm 1 \times 10^{-3}$ mm. The temperature inside the sample and ongoing strain were constantly monitored and recorded in 1 min intervals, which allowed for monitoring of dilatometric behavior of each specimen during the phase transition of water in the pores.

4. RESULTS AND DISCUSSION

The mineralogical composition and fabric (structure and texture) determine the rocks petrophysical properties. According to (Heimann and Sass, 1989) the pores are characteristic feature of almost all travertines. Choquette and Pray (1970) classified limestone porosity into fabric selective and non-fabric selected. The main macroporosity of SP(T) travertines is fenestral, which can achieve centimetric-size pores (further vugs). Direction of framework pores is parallel to the bedding structures. According to Lucia′s petrophysical classification of pores (Lucia, 1995) the fenestral porosity can be considered as separate vug porosity. SP(T) travertines represent facie which is termed as L_{mix}– laminated travertine with vugs and non-porous levels. For the open porosity according to Siegesmund and Snethlage (2010), the classification scheme applies, according to which rocks with a porosity of less than 1 % are considered compact rocks, with a porosity of 1 % to 2.5 % for rocks with low porosity from 5 % to 10 % for highly porous rocks and from 10 % to 20 % porosity are very porous rocks with a high number of pores. Based on the above classification scheme, SP(T) travertines can be classified as highly porous to very porous. From the laboratory determination of the internal structure of the pores by analyzing the results of effective porosity and total porosity we can state
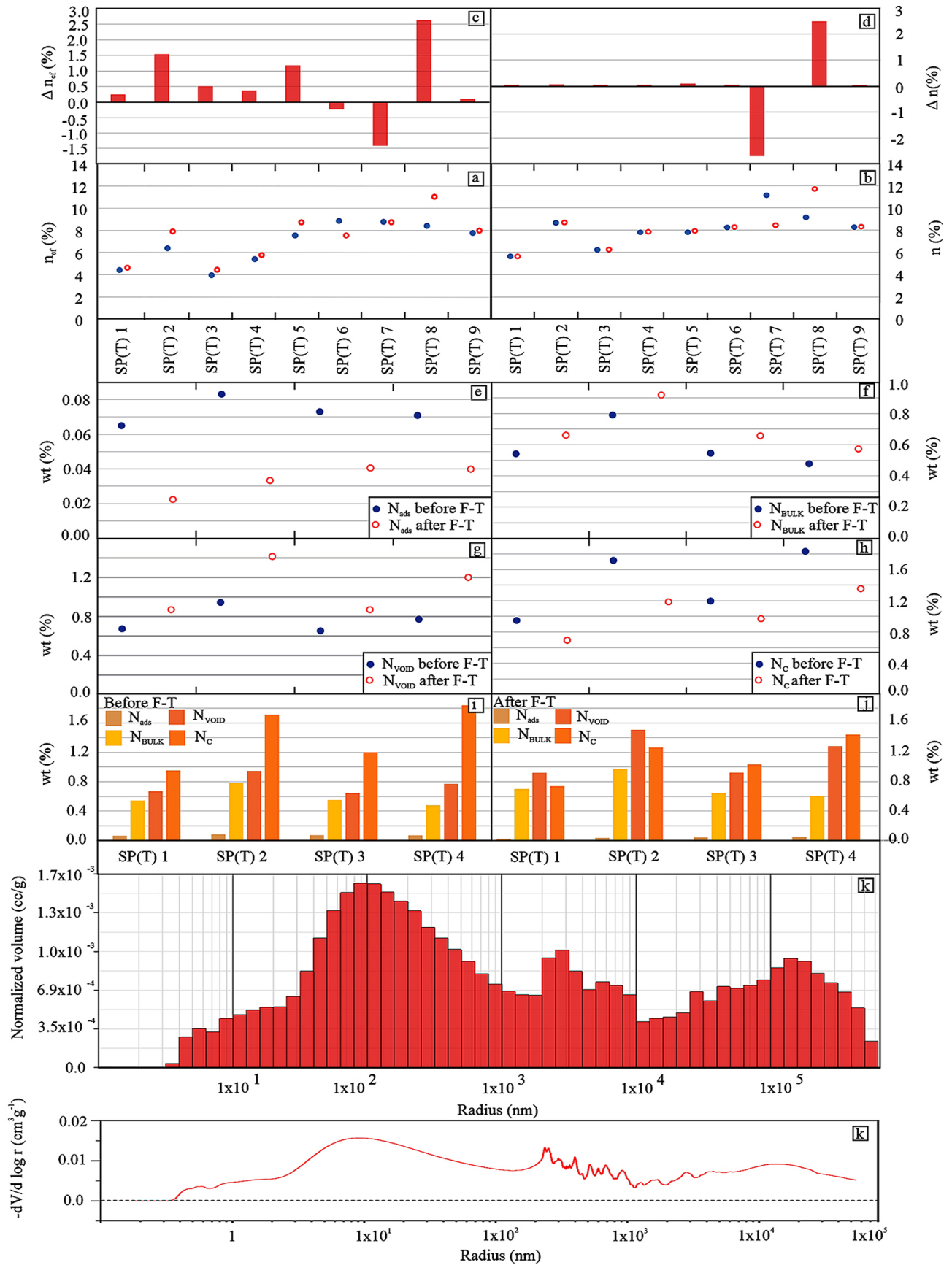
Fig. 5: Petrophysical properties before and after 100 F-T (freeze-thaw) cycles: a) effective porosity; b) total porosity; c,d) changes in effective and total porosity before and after 100 F-T (freeze-thaw) cycles; e,f,g,h,i,j) Nads; NBULK ;NVOID; NC from indicative rock pore structure method k1,k2) Pore Size Distribution from MIP
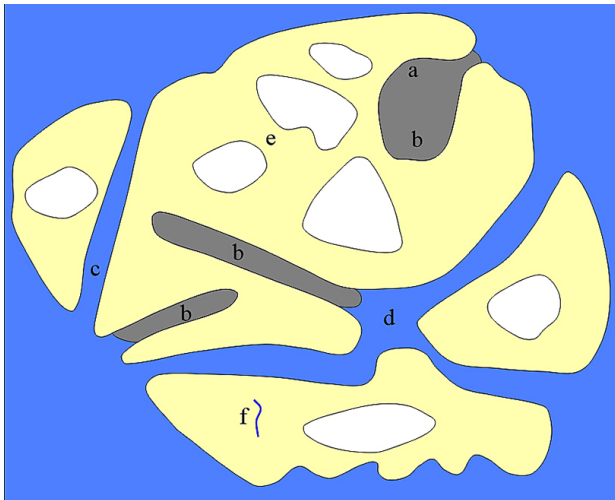
Fig. 6: Illustrated pore structure of the SP(T) travertine: Nvoid – inaccessible pores to water under standard conditions a) pores with narrow necks, b) blind pores; NBULK – pores easily accessible to water c) macropores d) network of macropores; NC – isolated pores not accessible to water- e; NADS – pores with adsorbed water by capillary condensation of air humidity f) micropores and mesopores (modified figure of Rouquerol (1994))

Fig. 7: Saturation degree before and after 100 F-T (freeze-thaw) cycles

that SP(T) travertines show extreme heterogeneity. The total porosity ranged from 4 % to 12 % with no significant changes after 100 F-T (freeze-thaw) cycles except SP(T) 7 sample with relative strong decrease of 2.5 % and, on the contrary SP(T) 8 specimen with significant increase about 2.5 %. Effective porosity also varies between 4 % and 12%. For samples with originally low effective porosity we can see a slight increase after cycling. The SP (T) 2 sample increase was maximal, while in the highly porous samples a insignificant decrease in effective porosity was recorded after the application of 100 F-T (freeze-thaw) cycles. According to mercury intrusion porosimetry (MIP) results their pore size distribution pattern is bimodal. Regarding the percentages of pores in the SP(T) samples, despite the significant macroscopically observable pores (vugs), the proportion of micro and mesopores dominates over macropores. This knowledge is crucial in terms of further understanding of the processes taking place inside the

sample during F-T (freeze-thaw) action. According to indicative rock structure method results SP(T) samples have a pore size distribution (PSD) typical for travertines. Their total porosity is 7.08 % (average value) which increased by 0.04 pp to 7.12 % after F-T (freeze-thaw) cycling. The largest volume is occupied by water-closed pores, namely the entire half of total pore volume, i.e. 50.1 %. The proportion of the pores easily accessible to water (20.7 %) and hardly accessible to water (26.6 %) differs only by case. The volume of pores hardly accessible to water is larger, which indicates an increased volume of blind pores and pores connected to environment by a narrow neck (ink-bobble pores). After 100 F-T (freeze-thaw) cycles the proportion of the individual pore categories changed significantly and consistently on all tested samples. The content of micropores and mesopores decreased only by 1.2 pp of the total porosity, i.e., a decrease by 1.4 pp. Closed pores, originally the dominant pores with their 50.1 % content lost their predominance and decreased by 13.4 pp to 36.8 %. The proportion of easily accessible pores
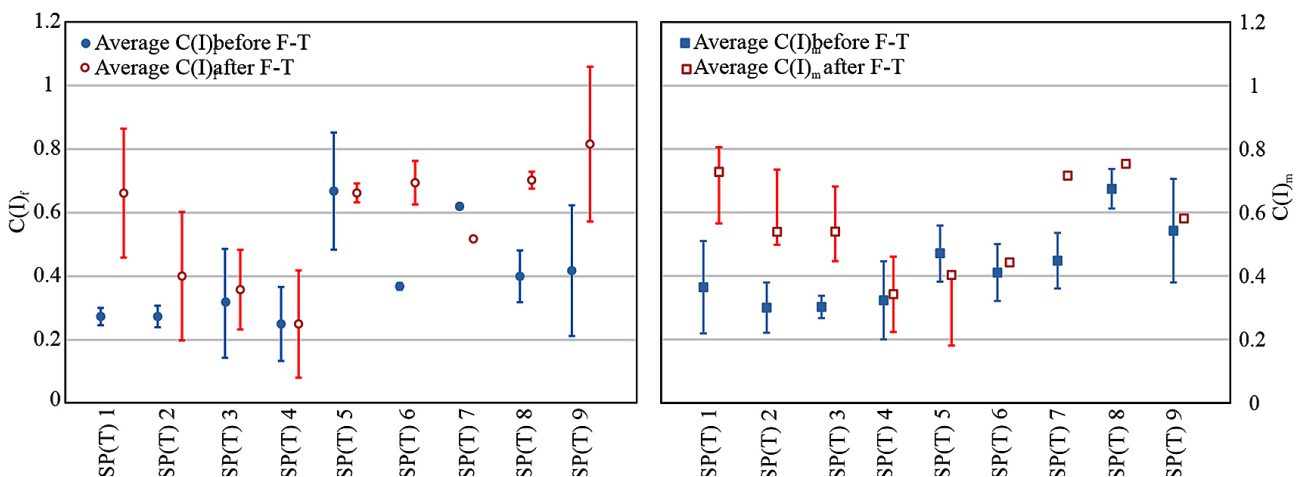
Fig. 8: Average imbition slopes recorded before and after 100 cycles of F-T (freeze-thaw) for fast (a) and medium (b) imbibition time window

▲ Imbibition after 100 F-T cycles   □ Initial imbibition
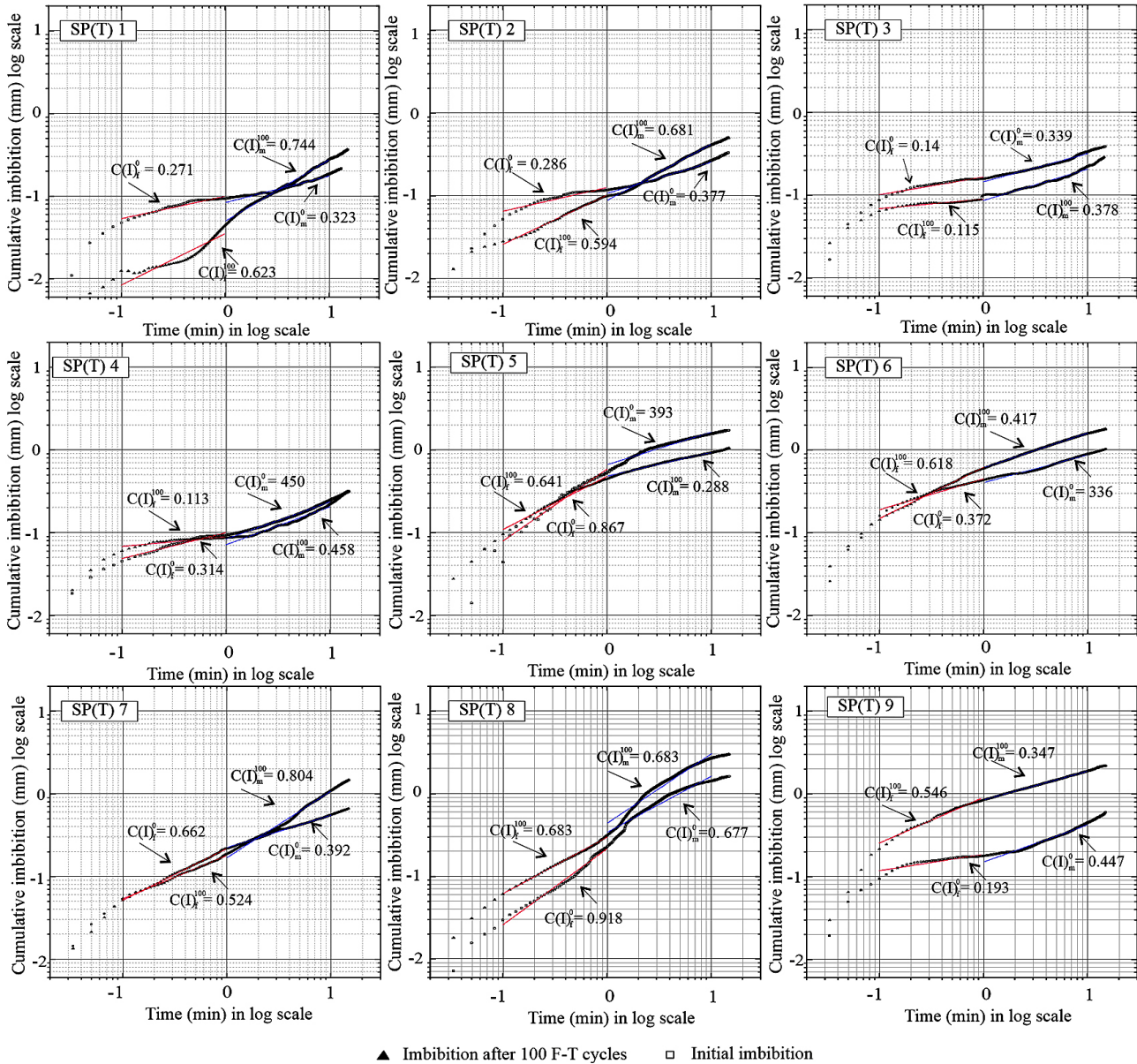
Fig. 9: Results from imbibition tests of SP(T) samples showing typical slopes of imbibition curves for fast (0.1-1min) and medium (1-10min) time intervals

and hardly accessible pores to water increased significantly. The proportion of easily accessible pores to water increased by 3.3 pp to 24.0 and the proportion of pores hardly accessible to water increased by 11.4 pp i. e., to 38.0 % (Fig. 5).

The total amount of absorbed water into the pore system is closely related to the porosity of the rock and was calculated as a saturation degree Sr (%) before and after 100 F-T (freeze-thaw) cycles with respect to the total water absorption under vacuum of the respective samples i.e. Sr (%) related to effective porosity (Fig. 7). The average initial saturation degrees of tested SP(T) travertines varies between 40 % and 90 %. In samples with a low degree of saturation (also lower porosity) the SP(T) 1 to SP(T) 4 Sr increased on average by 10 to 15 pp after cycling. On the contrary, in samples SP(T) 5 to SP(T) 9 the degree of saturation decreases, which correlates with a slight decrease in the porosity of these samples. Water transport by capillary imbibition reflects the pore size distribution and porosity.

Extreme heterogeneity in these properties was also reflected in the level of interconnection of the pore systems of the SP(T) samples. Samples SP(T) 1–4 had an initial average value of = 0.275, which increased by 51.5 pp to = 0.417 after F-T (freeze-thaw) cycles. An even larger boost in the imbibition rate was observed for the medium time interval, where = 0.321 grew by 67.3 pp to = 0.537 after testing in the thermodilatometer VLAP04 (Fig. 8). Samples SP(T) 5–9 had an initial average value of which increased by 37,2 pp to and initial = 0.508 with 14 % increase to = 0.579. Overall, SP(T) travertines have medium level of pore interconnectivity for both fast 0.1–1 min and medium 1–10 min time intervals (Fig. 8, Fig. 9).

This implies a slow advancement of the diffusion front in this rock type. The strain behavior due to ice crystallization of water-saturated samples is based on various pore system characteristics as the water content in rock pores, rock fabric and mineralogical composition.
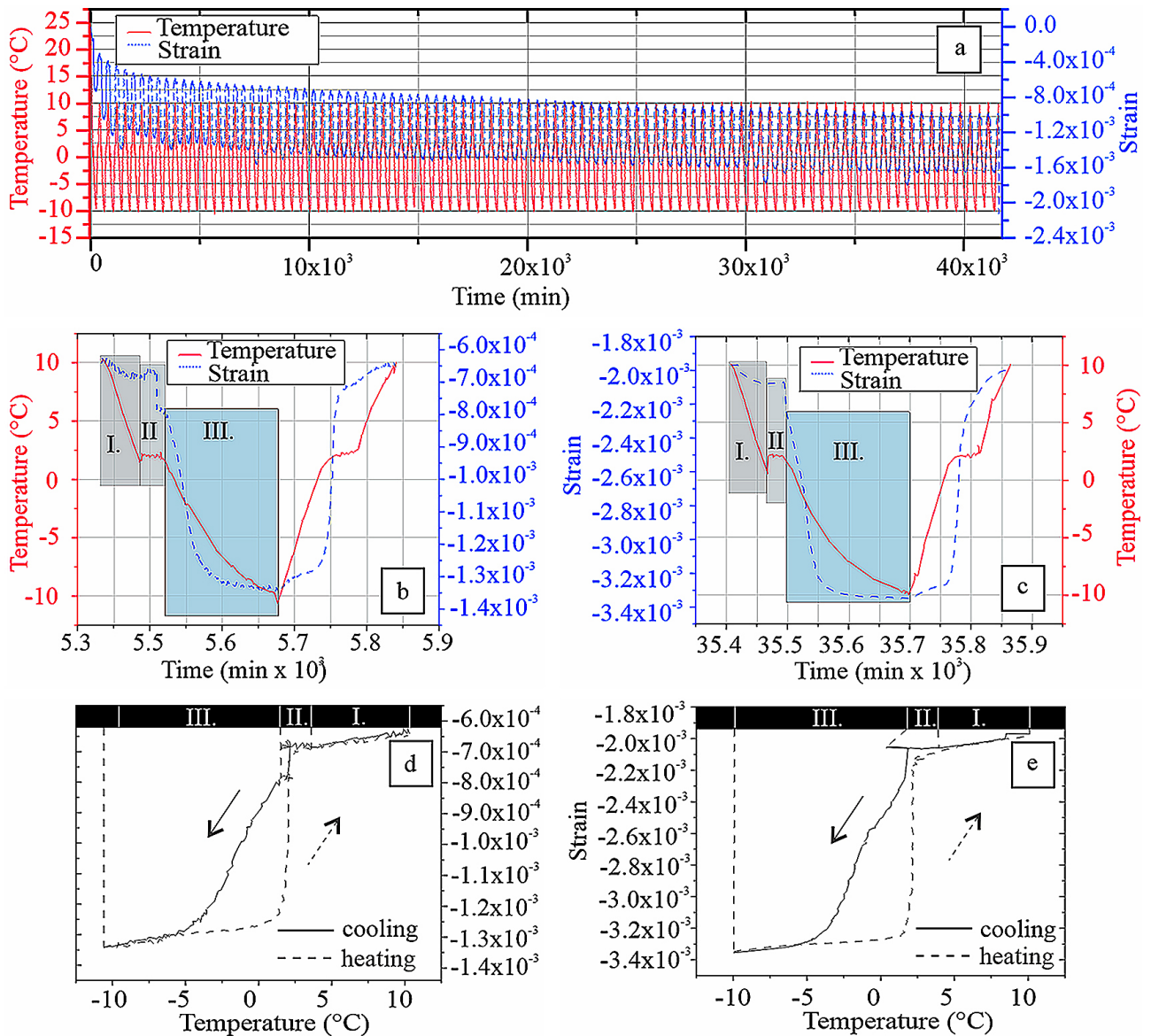
Fig. 10: Record of temperature and strain behavior of SP(T) samples; a) Temperature and strain path during 100 F-T (freeze-thaw) cycles, b,c) Detailed records of temperature and strain vs time during 14-th and 83-rd F-T (freeze-thaw) cycle; d,e) Detailed records of strain vs. temperature during 14-th and 83-rd F-T (freeze-thaw) cycle

The strain and temperature behavior during F-T (freeze-thaw) cycling is further plotted as strain versus time diagrams and divided into three characteristic zones- I., II., III (Fig. 10). Regarding the pattern of strain path for SP(T) travertines, the samples' general contraction is observed during cooling in Zone I. This process is not affected by the crystallization of ice in the rock pores yet. In zone II, a very weak expansion occurs around 0 °C and this expansion slightly decreases during the cycling for SP(T) 6 specimen. The expansion phenomenon may be traced back to an initial ice crystallization within the pore space. Crystallization of water is an exothermal process caused by the generation and diffusion of latent heat. This process is manifested by a temperature increase of approximately 2 °C. The temperature stays constant during the ice crystallization time (t_c) and resumes the decrease once the latent heat release has stopped. According to thermodynamic theories water freezes

at 0 °C in pores which are larger than 1μm. During ice crystallization a nanometer thick liquid layer between the crystal and the pore wall will cause that the crystal will exert pressure on the pore wall (Scherer, 1999). In the same time, water is drawn to the ice front (or crystals) by thermodynamical disequilibria. This causes a negative pore pressure in micro and mesopores, which means that the material is shrinking instead of expanding and that's explains a strong contraction of the sample in zone III.

The crystals at the ice front will however grow, leading to crystallization pressures to the ice front. Crystallization pressure can overcome the negative capillary pressures only when the thermodynamical equilibria are interrupted (Scherer and Valenza, 2005). In general terms, samples displayed heterogeneity in microstructural development of pores. This can be explained by complicated and heterogenous geometry and topology of the

SP(T) travertine pore spaces. Samples with a relative lower effective porosity and a relative lower level of pore interconnection also had a lower initial degree of saturation. This could subsequently be reflected in a different deterioration mechanism induced by ice crystallization in the pores. According to Everett (1961), it is more energetically favorable for ice crystals to form first in the larger pores, while the water in the smaller pores remains supercooled. As water crystallizes first in the larger pores of the system in a fast manner, the 9 % volume expansion causes part of the water in these larger pores to be forced out into the smaller neighboring pores. Hence, if this expelled water cannot find a pore large enough or pore interconnection is too low to relief this pressure, hydraulic pressures build up and can damage the material. The hydraulic together with the crystallization pressures in the larger pores thus cooperate in the overall weaking of the sample and thus result in microstructural evolution in terms of increase in effective porosity or pore interconnection. This phenomenon is referred by several authors as sub-critical crack growth (Chau and Shao, 2006; Ishikawa et al., 2004; Kemeny, 1991; Nicholson and Nicholson, 2000) or fatigue cracking (Griggs, 1936; Hall, 1999) in Deprez et al., (2020). However, the effect of frost shrinking caused by the reduction of pore pressures in micropores and mesopores is not overcome due to their predominance in pore size distribution pattern of SP(T) samples and total contraction of the samples after 100 F-T (freeze-thaw) cycles occurs. On the other hand in the samples, which had a higher initial effective porosity and at same time the level of pore interconnection, frost shrinking predominates because hydraulic pressures could be partially relieved which results in decrease of pore interconnection and effective porosity. Summarizing the results presented above, we can state, that SP(T) travertines are a relative resistant material in terms of frost weathering deterioration. However, outlined mechanisms of deterioration are still at the level of the hypothesis and need to be verified. In our future research, it will be necessary and decisive to focus on the analysis of the geometry and topology of the pore network by using non-destructive methods such as μCT scanning, by which we are able to visualize the pore network environment or simulate material properties such as absolute permeability in terms of its change after F-T cycling. Through comprehensive analysis of changes in petrophysical properties, dynamic monitoring of F-T cycles and non-destructive visualization of the pore environment, we will be able to verify previous hypotheses concerning heterogeneous materials such as travertines.

5. CONCLUSION

Frost weathering is important physical decay process which influences the structural performance of the degradation of hard rocks. In this study, experimental research was carried out focusing on the effects of repeated F-T cycles on rock petrophysical properties of travertine from Spišské Podhradie. Regarding the petrophysical properties: total porosity, effective porosity, pore size distribution and pore interconnection were performed before and after 100 F-T cycles as well as recorded strain path behavior and temperature development by a specially constructed thermodilatometer on vacuum-saturated samples. Based on the testing of 9 travertine specimens it can be stated:

Travertines from Spišské Podhradie belong to the L_{mix} facie of laminated travertines with vugs and non-porous levels. This structure causes a significant heterogeneity in their petrophysical properties.

• According to petrophysical classifications the microporosity is fenestral. Separated vugs up to a centimeter in size are parallel to the bedding structure. Its effective as well as total porosity is very variable and varies in a relatively wide range. The pore size distribution pattern is bimodal and level of pore interconnection is low to medium. The microstructural development induced by the ice crystallization within the pores reflects the high heterogeneity of these parameters, and thus defines the various failure mechanisms involved in the overall deterioration of the rock material due to frost weathering.

• Crystallization and hydraulic pressures cooperate in rock failure, but they are not sufficient to overcome the reduction of pores pressures in the micro and mesopores of the rock, therefore instead of the overall expansion of the specimen, a contraction occurs. The intensity of these processes seems to be controlled mainly by the level of pore interconnectivity.

• Overall, travertines from Spišské Podhradie does not show any macroscopically observable changes caused by frost weathering. Based on the extent of changes in the microstructure of the rock after the application of 100 F-T cycles we can state that travertines from Spišské Podhradie are rather resistant to the effects of F-T action on the pore system of the rock.

References:

Adamcova R., 2012: Open porosity assessment of the rocks using helium pycnometer. *Geotechnika*, 15, 4, 26–31. [In Slovak]

Benavente D., Martinez-Martinez J., Cueto, N., Ordonez S., Garcia-del-Cura M. A., 2018: Impact of salt and frost weathering on the physical and durability properties of travertines and carbonate tufas used as building material. *Environmental Earth Science*, 77, 147, 1–13.

Chau K.T., Shao J.F., 2006: Subcritical crack growth of edge and center cracks in façade rock panels subject to periodic surface temperature variations. *Int. J. Solids Struct*, 43, 807–827.

Chentout M., Allou B., Rezouk A., Belhai D., 2015: Experimental study to evaluate the effect of travertine structure on the physical and mechanical properties of the material. *Arab. J. Geosci.* 8, 8975–8985.

Choquette P.W., Pray L.C., 1970: Geology nomenclature and classsification of porosity in sedimentary carbonates. *AAPG Bull.*, 54, 207–250.

De Kock T., Boone M. A., De Schryver T., Van Stappen J., Derluyn H., Masschaele B., De Schutter G., Cnudde V., 2015: A Pore-scale study of fracture dynamics in rock using X-ray micro- CT under ambient freeze–thaw cycling. *Environ. Sci. Technol.*, 49, 2867–2874.

Demirdag S., 2013: Effects of freezing–thawing and thermal shock cycles on physical and mechanical properties of filled and unfilled travertines. *Constr. Build. Mater.*, 47, 1395–1401.

Deprez M., De Kock T., De Schutter G., Cnudde V., 2020: A review on freeze-thaw action and weathering of rocks. *Earth Science-Review,* 203, 103143.

Dunn J. R., Hudec P. P., 1966: Water, clay and rock soundness. *Ohio J. Sci.,* 66, 2, 153–167.

Everett D. H., 1961: Thermodynamics of frost damage to porous solids. *Trans. Faraday Soc.,* 57, 7, 1541–1551.

Everett D. H., Haynes J. M., 1965: Capillary properties of some model pore systems with special references to frost damage. Re-Union Internationale des Laboratoires d´Essois et de Recherches sur les Matereaux et les Constructions, R.I.L.E.M. Bull New Ser. 27, 31–38.

Griggs, D. T., 1936: The factor of Fatigue in Rock Exfoliation. *J. Geol.,* 44, 783–796.

Grossi C. M., Brimblecombe P., Harris I., 2007: Predicting long term freeze-thaw risks on Europe built heritage and archaeological sites in a changing climate. *Sci. Total Environ*, 377, 2–3, 273–281.

Hall K., 1999: The role of thermal stress fatigue in the breakdown of rock in cold regions. *Geomorphology*, 31, 47–63.

Handy L. L., 1960: Determination of Effective Capillary Pressures for Porous Media from Imbibition Data. *Trans.,* 219, 75–80.

Heimann A., Sass E., 1989: Travertines of the northern Hula Valley, Israel. *Sedimentology*, 36, 95–108.

Hirschwald J., 1908: Die Prüfung der naturlichen Bausteine auf ihre Verwitterungsbeständigkeit. Verlag Wilhelm Ernst & Sohn, Berlin, 144 p. [In German]

Hu Q., Persoff P., Wang J. S. Y., 2001: Laboratory measurement of water imbibition into low- permeability welded tuff. *J. Hydrol.,* 242, 64–78.

Ishikawa M., Kurashige Y., Hirakawa K., 2004: Analysis of crack movements observed in an alpine bedrock cliff. *Earth Surf. Process. Landf.,* 29, 883–891.

Kemeny J. M., 1991: A model for non-linear rock deformation under compression due to sub-critical crack growth. *Int. J. Rock Mech. Min. Sci. Geomech. Abstr.,* 28, 459–467.

Lucia F. J., 1995: Rock-fabric petrophysical classification of carbonate pore-space for reservoir characterization. *AAPG Bull.,* 79, 1275–1300.

McGreevy J. P., Whalley W. B., 1982: The geomorphic significance of rock temperature variations on cold environments: A discussion. *Arct. Antarct. Alp. Res.,* 14, 2, 157–162.

Nakamura K., Jacob K. H., Davies J. N., 1977: Volcanoes as possible indicators of tectonics stress orientation - Aleutians and Alaska. *Pure Appl. Geophys.,* 115, 87–112.

Nicholson D. T., Nicholson F. H., 2000: Physical deterioration of sedimentary rocks subjected to experimental freeze-thaw weathering. *Earth Surf. Process. Landf.,* 25, 1295–1307.

Nye J. F., 1972: Physical properties of Crystals. Oxford University Press, London, 329 p.

Ondrasik M., Kopecky M., Brcek M., 2017: Nasiakavosť hornín určená za rôznych podmienok ako alternatívny identifikátor štruktúry horninových pórov a mrazuvzdornosti. In: Datel J. V., Tomášek J. (Eds.): Podzemní voda a společnost, sborník příspěvků XV. hydrogeologického kongresu, Brno. [In Slovak]

Ondrasik M., Frankovska J., Kopecky M., Brcek M., 2018: Simple Method of Rock Pore Structure Determination Presented with the Most Common Rock Types Quarried in Slovakia. In: L. Laloui, A. Ferrari, Energy Geotechnics: SEG-2018, Springer, pp. 299–306.

Operator Manual – STEREOPYCNOMETER. Boynton Beach, FL, USA, Quantachrome Instruments 2005. 14 p.

Pentecost A., 2005: Travertine. Springer-Verlag Berlin, Heidelberg, 445 p.

Powers T. C., 1945: A Working hypothesis for further studies of frost resistance of concrete. In: Journal Proceedings- American Concrete Institute, 245 p.

Powers, T.C., 1949. The air requirement of frost resistant concrete. Highw. Res. Board Proc. 29, 184–211.

Prick A., 1995: Dilatometrical behaviour of porous calcareous rock samples subjected to freeze - thaw cycles. *Catena*, 25, 7–20.

Rouqerol J., Avnir D., Fairbridge W.C., Everett D.H., Haynes J.H., Pernicone N., Ramsay J.D.F., Sing K.S.W., 1994: Recommendations for characterization of porous solids, Pure & Appl. Chern., Vol. 66, No. 8, pp. 1739–1758, 1994

Ruedrich J., Kirchner D., Siegesmund S., 2011: Physical weathering of building stones induced by freeze–thaw action: a laboratory long-term study. *Environ. Earth Sci.,* 63, 1573–1586.

Ruedrich J., Siegesmund S., 2007: Salt and ice crystallisation in porous sandstones. *Environ. Geol.,* 52, 225–249.

Siegesmund S., Snethlage R., 2010: Stone in Architecture: Properties, Durability. 4th ed. Springer, Berlin, Heidelberg, 552 p.

Sing K. S. W., Everett D. H., Haul R. A. W., Moscou L., Pierotti R. A., Rouquérol J., Siemieniewska T., 1985: Reporting Physisorption Data for Gas/Solid Systems With Special Reference to the Determination of Surface Area and Porosity. *Pure Appl. Chem.,* 57, 603.

Scherer G. W., 1999: Crystallization in pores. *Cem. Concr. Res.,* 29, 1347–1358.

Scherer G. W., Valenza J .J., 2005: Mechanisms of frost damage. Mater. Sci. Concr. VII, 209–246.

Steiger M., 2005[a]: Crystal growth in porous materials – I, The crystallization pressure of large crystals. *J. Cryst. Growth.,* 282, 455–469.

Steiger M., 2005[b]: Crystal growth in porous materials – II, The crystallization pressure of large crystals. *J. Cryst. Growth.,* 282, 470–481.

STN 72 1011 (1982) Laboratory determination of apparent density of solid particles of soils.

STN EN 13755 (2003) Natural stone test methods. Determination of water absorption at atmospheric pressure.

STN EN 1936 (2007) Natural stone test methods. Determination of real density and apparent density, and of total and open porosity.

Walder J., Hallet B., 1985: A theoretical model of the fracture of rock during freezing. *Geol. Soc. Am. Bull.,* 96, 3, 336–346.

Weast R. C., 1973: Hand Book of Chemistry and Physics, CRC, 54th ed. Cleveland, 1973.

Winkler E. M., 1968: Frost damage to stone and concrete: geological considerations. *Eng. Geol.,* 2, 315–323.

Yavuz A. B., Topal T., 2007: Thermal and salt crystallisation effects on marble deterioration: examples from Western Anatolia, Turkey. *Eng. Geol.,* 90, 30–40.

Yu S., Oguchi C. T., 2010: Role of pore size distribution in salt uptake, damage, and predicting salt susceptibility of eight types of Japanese building stones. *Eng. Geol.,* 115, 226–236.

Zalooli A., Khamehchiyan M., Nikudel M. R., Jamshidi A., 2017: Deterioration of travertine samples due to magnesium sulfate crystallisation pressure: examples from Iran. *Geotech. Geol. Eng.,* 35, 463–473.